

## Probing the Interactions of O<sub>2</sub> with Small Gold Cluster Anions (Au<sub>n</sub><sup>−</sup>, *n* = 1–7): Chemisorption vs Physisorption

Wei Huang, Hua-Jin Zhai, and Lai-Sheng Wang\*

Department of Chemistry, Brown University, Providence, Rhode Island 02912

Received December 9, 2009; E-mail: lai-sheng\_wang@brown.edu

**Abstract:** Activation of O<sub>2</sub> is the most critical step in catalytic oxidation reactions involving gold and remains poorly understood. Here we report a systematic investigation of the interactions between O<sub>2</sub> and small gold cluster anions Au<sub>n</sub><sup>−</sup> (*n* = 1–7) using photoelectron spectroscopy. Higher resolution photoelectron spectra are obtained for the molecularly chemisorbed even-sized Au<sub>n</sub>O<sub>2</sub><sup>−</sup> (*n* = 2, 4, 6) complexes. Well-resolved vibrational structures due to O–O stretching are observed and can be readily distinguished from the Au-derived PES bands. The adiabatic detachment energies and O–O vibrational frequencies are measured to be 3.03 ± 0.04, 3.53 ± 0.05, and 3.17 ± 0.05 eV, and 1360 ± 80, 1360 ± 80, and 1330 ± 80 cm<sup>−1</sup> for *n* = 2, 4, 6, respectively. Physisorbed Au<sub>n</sub><sup>−</sup>(O<sub>2</sub>) complexes for *n* = 1, 3, 5, 7 are observed for the first time, providing direct evidence for the inertness of the closed-shell odd-sized Au<sub>n</sub><sup>−</sup> clusters toward O<sub>2</sub>. Neutral even-sized Au<sub>n</sub> clusters are closed-shell and are expected to be inert toward O<sub>2</sub>, which is not consistent with the reduced O–O vibrational frequencies observed in the photoelectron spectra relative to free O<sub>2</sub>. It is suggested that the photodetachment transitions can only access excited states of the neutral even-sized Au<sub>n</sub>O<sub>2</sub> complexes; a double-well potential is proposed consisting of the ground-state van der Waals well at long Au<sub>n</sub>–O<sub>2</sub> distances and a higher energy deeper well at short Au<sub>n</sub>–O<sub>2</sub> distances derived from singlet O<sub>2</sub> (<sup>1</sup>Δ<sub>g</sub>). The current study provides further insight into O<sub>2</sub> interactions with small gold clusters, as well as accurate experimental data to benchmark theoretical investigations.

### 1. Introduction

The reactivity of gold clusters with O<sub>2</sub> is important for understanding the remarkable catalytic effects discovered for gold nanoparticles.<sup>1</sup> Bulk gold surfaces are known to be inactive toward O<sub>2</sub>,<sup>2</sup> and thus O<sub>2</sub> activation is believed to be the main rate-limiting step in nanogold catalysis. While both anionic and cationic Au species have been proposed as active sites in nanogold catalysis,<sup>3–6</sup> recent experimental evidence suggests that the catalytic active sizes for CO oxidation may involve subnanometer gold particles containing only about 10 Au atoms.<sup>7</sup> Unsupported nanosized Au particles have also been shown to be active catalysts,<sup>8,9</sup> suggesting that the catalytic

activity may be intrinsic to the nano- or subnanogold particles. A critical question pertaining to nanogold catalysis is whether and how gold nanoparticles interact with and activate molecular oxygen.

Size-selected gas phase clusters can serve as well-defined and controllable models for mechanistic understandings of nanogold catalysis at the molecular level.<sup>10–19</sup> Early reactivity studies of Au<sub>n</sub><sup>−</sup> toward O<sub>2</sub> revealed molecular O<sub>2</sub> addition as the primary reaction channel only for the even-sized clusters, whereas the odd-sized clusters are inert toward O<sub>2</sub>.<sup>10</sup> The even–odd alterna-

- (1) Haruta, M. *Catal. Today* **1997**, *36*, 153.
- (2) Gottfried, J. M.; Schmidt, K. J.; Schroeder, S. L. M.; Christmann, K. *Surf. Sci.* **2002**, *511*, 65.
- (3) (a) Sanchez, A.; Abbet, S.; Heiz, U.; Schneider, W. D.; Hakkinen, H.; Barnett, R. N.; Landman, U. *J. Phys. Chem. A* **1999**, *103*, 9573. (b) Yoon, B.; Hakkinen, H.; Landman, U.; Worz, A. S.; Antonietti, J. M.; Abbet, S.; Judai, K.; Heiz, U. *Science* **2005**, *307*, 403.
- (4) Yan, Z.; Chinta, S.; Mohamed, A. A.; Fackler, J. P., Jr.; Goodman, D. W. *J. Am. Chem. Soc.* **2005**, *127*, 1604.
- (5) (a) Guzman, J.; Gates, B. C. *J. Am. Chem. Soc.* **2004**, *126*, 2672. (b) Fierro-Gonzalez, J. C.; Bhirud, V. A.; Gates, B. C. *Chem. Commun.* **2005**, 5275.
- (6) Fu, Q.; Saltsburg, H.; Flytzani-Stephanopoulos, M. *Science* **2003**, *301*, 935.
- (7) Herzing, A. A.; Kiely, C. J.; Carley, A. F.; Landon, P.; Hutchings, G. J. *Science* **2008**, *321*, 1331.
- (8) Iizuka, Y.; Tode, T.; Takao, T.; Yatsu, K. I.; Takeuchi, T.; Tsubota, S.; Haruta, M. *J. Catal.* **1999**, *187*, 50.
- (9) Xu, C.; Su, J.; Xu, X.; Liu, P.; Zhao, H.; Tian, F.; Ding, Y. *J. Am. Chem. Soc.* **2007**, *129*, 42.
- (10) (a) Cox, D. M.; Brickman, R. O.; Creagan, K.; Kaldor, A. Z. *Phys. D* **1991**, *19*, 353. (b) Lee, T. H.; Ervin, K. M. *J. Phys. Chem.* **1994**, *98*, 10023. (c) Salisbury, B. E.; Wallace, W. T.; Whetten, R. L. *Chem. Phys.* **2000**, *262*, 131.
- (11) (a) Hagen, J.; Socaciu, L. D.; Eljazyfer, M.; Heiz, U.; Bernhardt, T. M.; Woste, L. *Phys. Chem. Chem. Phys.* **2002**, *4*, 1707. (b) Bernhardt, T. M. *Int. J. Mass Spectrom.* **2005**, *243*, 1.
- (12) Wallace, W. T.; Whetten, R. L. *J. Am. Chem. Soc.* **2002**, *124*, 7499.
- (13) Socaciu, L. D.; Hagen, J.; Bernhardt, T. M.; Woste, L.; Heiz, U.; Hakkinen, H.; Landman, U. *J. Am. Chem. Soc.* **2003**, *125*, 10437.
- (14) (a) Stolcic, D.; Fischer, M.; Gantefor, G.; Kim, Y. D.; Sun, Q.; Jena, P. *J. Am. Chem. Soc.* **2003**, *125*, 2848. (b) Kim, Y. D.; Fischer, M.; Gantefor, G. *Chem. Phys. Lett.* **2003**, *377*, 170.
- (15) Sun, Q.; Jena, P.; Kim, Y. D.; Fischer, M.; Gantefor, G. *J. Chem. Phys.* **2004**, *120*, 6510.
- (16) Kimble, M. L.; Castleman, A. W., Jr.; Mitric, R.; Burgel, C.; Bonacic-Koutecky, V. *J. Am. Chem. Soc.* **2004**, *126*, 2526.
- (17) Fielicke, A.; von Helden, G.; Meijer, G.; Pedersen, D. B.; Simard, B.; Rayner, D. M. *J. Am. Chem. Soc.* **2005**, *127*, 8416.
- (18) (a) Zhai, H. J.; Wang, L. S. *J. Chem. Phys.* **2005**, *122*, 051101. (b) Zhai, H. J.; Kiran, B.; Dai, B.; Li, J.; Wang, L. S. *J. Am. Chem. Soc.* **2005**, *127*, 12098.
- (19) (a) Neumaier, M.; Weigend, F.; Hampe, O.; Kappes, M. M. *J. Chem. Phys.* **2005**, *122*, 104702. (b) Neumaier, M.; Weigend, F.; Hampe, O.; Kappes, M. M. *Faraday Discuss.* **2008**, *138*, 393.

tion correlates well with a similar trend in the electron affinities of Au<sub>*n*</sub>,<sup>20</sup> suggesting that electron transfer from Au<sub>*n*</sub><sup>−</sup> to O<sub>2</sub> might be the primary reaction mechanism.<sup>10c</sup> In subsequent photoelectron spectroscopy (PES) studies,<sup>14,15</sup> spectroscopic evidence was reported, showing that the even-sized Au<sub>*n*</sub>O<sub>2</sub><sup>−</sup> clusters are indeed molecularly chemisorbed complexes via the observation of O–O vibrational structures, with estimated vibrational spacings ranging from ~180 meV (1450 cm<sup>−1</sup>) for *n* = 2 and 6 to 152 meV (1230 cm<sup>−1</sup>) for *n* = 4.

There have been numerous theoretical investigations on the reactivity of gold clusters with O<sub>2</sub>. While most theoretical studies show the even–odd effect for the anion clusters, consistent with the experimental observations, the situation for the neutral clusters is more complicated because there is a lack of direct experimental probe for the uncharged species. Several previous density functional theory (DFT) studies show persistently that neutral Au clusters interact with O<sub>2</sub> rather weakly, insufficient to activate molecular oxygen.<sup>21,22</sup> Specifically, Landman and co-workers<sup>21</sup> concluded that, despite the weak binding to O<sub>2</sub>, neutral and cationic Au clusters do not induce O–O bond activation. Jena and co-workers<sup>15</sup> showed that in neutral Au<sub>2</sub>O<sub>2</sub> and Au<sub>4</sub>O<sub>2</sub> clusters electron transfer takes place from O<sub>2</sub> to Au<sub>2</sub> and Au<sub>4</sub> owing to the high electronegativity of Au. Ding et al.<sup>22</sup> showed that there is no O<sub>2</sub> chemisorption in the Au<sub>*n*</sub>O<sub>2</sub> (*n* = 2, 4, 6) neutral complexes, and thus their O–O stretching frequencies should be close to or almost the same as that in free O<sub>2</sub> (1580 cm<sup>−1</sup>). *Ab initio* calculations by the groups of Gordon and Metiu showed that while O<sub>2</sub> has a 1.07 eV binding energy to Au<sub>2</sub><sup>−</sup> it only weakly interacts with either Au<sub>3</sub><sup>−</sup> or Au<sub>3</sub>.<sup>23</sup> They showed that DFT methods can give rise to large errors in predicting the O<sub>2</sub> binding to gold clusters.

However, the consistent theoretical predictions of weak binding between O<sub>2</sub> and neutral gold clusters do not agree with the observed vibrational structures in the PES spectra of even-sized Au<sub>*n*</sub>O<sub>2</sub><sup>−</sup> (*n* = 2, 4, 6) complexes.<sup>14</sup> Since PES probes the final neutral states, the observed vibrational structures should be due to the O–O vibration in the *neutral* Au<sub>*n*</sub>O<sub>2</sub> (*n* = 2, 4, 6) complexes. The reduced O–O frequencies relative to free O<sub>2</sub> in the PES spectra are puzzling. Clearly, there is something significant that is not well understood about the O<sub>2</sub> interactions with small gold clusters. High-quality spectroscopic data are needed to provide further insight.

In the current article, we report a systematic PES study of the Au<sub>*n*</sub>O<sub>2</sub><sup>−</sup> (*n* = 1–7) complexes for both the even- and odd-sized clusters. For the even-sized clusters (*n* = 2, 4, 6), significantly better resolved spectra are obtained and the possible mechanisms for the observed reduced O–O frequencies are discussed. For the odd-sized clusters (*n* = 1, 3, 5, 7), physisorbed Au<sub>*n*</sub><sup>−</sup>(O<sub>2</sub>) complexes are observed for the first time and their PES spectra are nearly identical to those of the parent Au<sub>*n*</sub><sup>−</sup> clusters, providing direct spectroscopic evidence for the inertness of these clusters toward O<sub>2</sub>. For AuO<sub>2</sub><sup>−</sup> and Au<sub>3</sub>O<sub>2</sub><sup>−</sup>, both the dioxide forms and the O<sub>2</sub> complexes are observed when an O<sub>2</sub>/He carrier gas is used, whereas only the dioxide forms are

observed when a N<sub>2</sub>O/He carrier gas is used. The current results provide further insight into the mechanisms of O<sub>2</sub> activation by small gold clusters and can be used to benchmark high-level computational studies on the interactions of O<sub>2</sub> with Au clusters.

## 2. Experimental Method

The experiment was carried out using a magnetic-bottle PES apparatus equipped with a laser vaporization cluster source, details of which have been described previously.<sup>24</sup> Briefly, the Au<sub>*n*</sub>O<sub>2</sub><sup>−</sup> cluster complexes were produced by laser vaporization of a pure Au disk target in the presence of a He carrier gas seeded with different amounts of O<sub>2</sub> and analyzed using a time-of-flight mass spectrometer. The Au<sub>*n*</sub>O<sub>2</sub><sup>−</sup> (*n* = 1–7) clusters of current interest were each mass-selected and decelerated before being photodetached. The photodetachment experiments were performed at three photon energies: 355 nm (3.496 eV), 266 nm (4.661 eV), and 193 nm (6.424 eV). Effort was made to control cluster temperatures and to choose colder clusters for photodetachment, which has proved essential for obtaining high-quality PES data.<sup>25</sup> Photoelectrons were collected at nearly 100% efficiency by the magnetic bottle and analyzed in a 3.5 m long electron flight tube. The experiment was run at 20 Hz repetition rate with the cluster beam off at alternating laser shots for background subtraction. Photoelectron time-of-flight spectra were converted to kinetic energy (*E<sub>k</sub>*) spectra, calibrated using the known spectra of Au<sup>−</sup> and Rh<sup>−</sup>. The reported electron-binding energy spectra were obtained by subtracting the kinetic energy spectra from the respective photon energies. The energy resolution of the PES apparatus was Δ*E<sub>k</sub>*/*E<sub>k</sub>* ≈ 2.5%, that is, ~25 meV for 1 eV electrons.

We found that in our cluster source the cluster distributions depended strongly on the O<sub>2</sub> content in the He carrier gas. At 0.1% O<sub>2</sub>, we observed only Au<sub>*n*</sub>O<sub>2</sub><sup>−</sup> complexes with even *n* in the size range of *n* = 2–8, consistent with previous studies.<sup>10,14</sup> At 0.5% O<sub>2</sub>, we found that most of the even-sized Au<sub>*n*</sub><sup>−</sup> clusters were converted to the Au<sub>*n*</sub>O<sub>2</sub><sup>−</sup> complexes. At the same time, more extensive O-containing clusters (Au<sub>*n*</sub>O<sub>*x*</sub><sup>−</sup>) were observed, including odd-numbered *n* and *x*. At 5% O<sub>2</sub>, we observed nearly continuous cluster distributions of Au<sub>*n*</sub>O<sub>*x*</sub><sup>−</sup> in both *n* and *x* due to extensive oxidation and complex formation. Most of our PES experiments were done using the 0.5% O<sub>2</sub>/He carrier gas. For AuO<sub>2</sub><sup>−</sup>, we used 5% O<sub>2</sub>/He carrier gas to enhance its intensity. We also used N<sub>2</sub>O%-seeded He carrier as the O source and were able to observe AuO<sub>2</sub><sup>−</sup> and Au<sub>3</sub>O<sub>2</sub><sup>−</sup>, which were compared with the results from the O<sub>2</sub>-seeded carrier gas.

## 3. Results

**3.1. Au<sub>n</sub>O<sub>2</sub><sup>−</sup> (*n* = 2, 4, 6).** The PES spectra of Au<sub>*n*</sub>O<sub>2</sub><sup>−</sup> (*n* = 2, 4, 6) at 193 nm are compared with those of the corresponding bare Au<sub>*n*</sub><sup>−</sup> clusters in Figure 1. Higher resolution spectra at 266 nm for Au<sub>*n*</sub>O<sub>2</sub><sup>−</sup> are shown in Figure 2. The new data are consistent with the previous reports by Gantefor and co-workers,<sup>14</sup> but are better resolved. In the 193 nm spectra (Figure 1), weak and broad features are observed in the low binding energy side, which come primarily from detachment from the O<sub>2</sub><sup>−</sup> unit in Au<sub>*n*</sub>O<sub>2</sub><sup>−</sup>. The relatively sharp features at higher binding energies (>4.8 eV) originate from the Au cluster substrates. At 266 nm (Figure 2), only the O<sub>2</sub>-derived bands are observed, which are resolved into different vibrational progressions. In the 266 spectrum of Au<sub>2</sub>O<sub>2</sub><sup>−</sup> (Figure 2a), three vibrational progressions (X, A, B) are resolved with frequencies

(20) Taylor, K. J.; Pettiette-Hall, C. L.; Cheshnovsky, O.; Smalley, R. E. *J. Chem. Phys.* **1992**, *96*, 3319.

(21) Yoon, B.; Hakkinen, H.; Landman, U. *J. Phys. Chem. A* **2003**, *107*, 4066.

(22) (a) Ding, X.; Li, Z.; Yang, J. L.; Hou, J. G.; Zhu, Q. *J. Chem. Phys.* **2004**, *120*, 9594. (b) Ding, X.; Dai, B.; Yang, J. L.; Hou, J. G.; Zhu, Q. *J. Chem. Phys.* **2004**, *121*, 621.

(23) (a) Varganov, S. A.; Olson, R. M.; Gordon, M. S.; Metiu, H. *J. Chem. Phys.* **2003**, *119*, 2531. (b) Mills, G.; Gordon, M. S.; Metiu, H. *Chem. Phys. Lett.* **2002**, *359*, 493.

(24) Wang, L. S.; Cheng, H. S.; Fan, J. *J. Chem. Phys.* **1995**, *102*, 9480.

(25) (a) Wang, L. S.; Li, X. In *Clusters and Nanostructure Interfaces*; Jena, P.; Khanna, S. N.; Rao, B. K., Eds.; World Scientific: NJ, 2000; pp 293–300. (b) Akola, J.; Manninen, M.; Hakkinen, H.; Landman, U.; Li, X.; Wang, L. S. *Phys. Rev. B* **1999**, *60*, R11297.

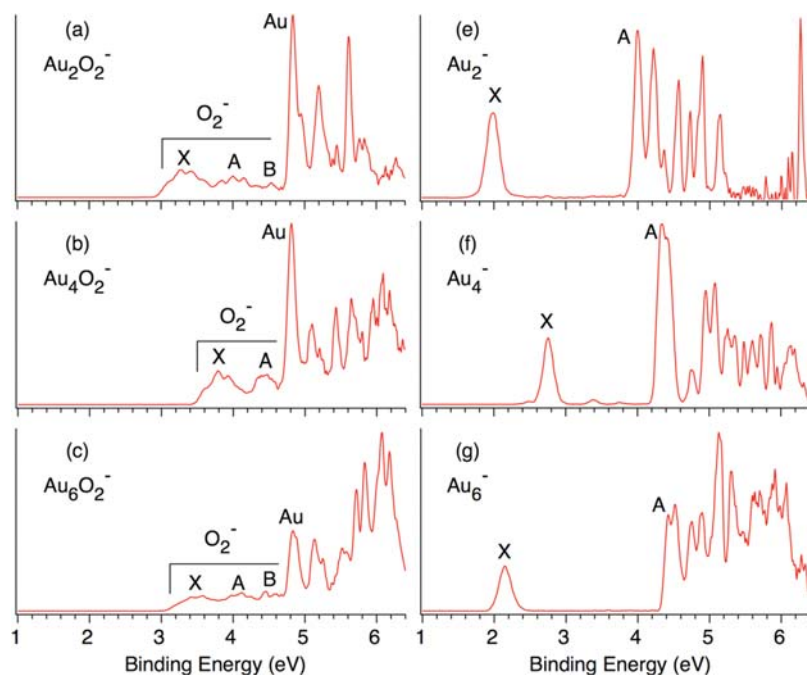


**Figure 1.** Photoelectron spectra of even-sized  $\text{Au}_n\text{O}_2^-$  ( $n = 2, 4, 6$ ) at 193 nm (6.424 eV) in comparison with those of the corresponding  $\text{Au}_n^-$  clusters.

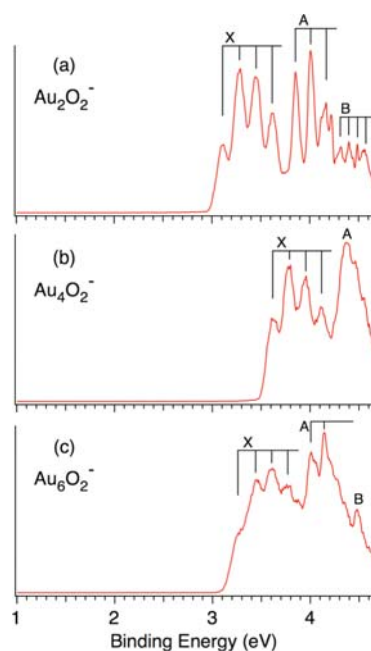


**Figure 2.** Photoelectron spectra of  $\text{Au}_n\text{O}_2^-$  ( $n = 2, 4, 6$ ) at 266 nm (4.661 eV). Resolved vibrational structures are labeled.

of 1360, 1250, and  $\sim 700\text{ cm}^{-1}$ , respectively. In the 266 nm of  $\text{Au}_4\text{O}_2^-$  (Figure 2b), two bands are observed, where the X band is vibrationally resolved. For  $\text{Au}_6\text{O}_2^-$  (Figure 2c), three bands are observed and vibrational structures are resolved in the X and A bands. The B band in the spectra of  $\text{Au}_2\text{O}_2^-$  and  $\text{Au}_2\text{O}_6^-$  was not identified in the previous study due to lower spectral resolution and poor signal-to-noise ratios.<sup>14</sup> However, because of the photon energy cutoff at 266 nm and the difficulty in detecting low-energy electrons by the magnetic-bottle PES analyzer, the spectral intensity above 4.5 eV in Figure 2 is not reliable. Nevertheless, as will be discussed in Section 4.2, the  $\text{O}_2$ -derived spectral features in  $\text{Au}_n\text{O}_2^-$  ( $n = 2, 4, 6$ ) resemble

**Table 1.** Observed Adiabatic (ADE) and Vertical (VDE) Detachment Energies and O–O Vibrational Frequencies from the PES Spectra of  $\text{Au}_n\text{O}_2^-$  ( $n = 2, 4, 6$ )<sup>a</sup>

	feature	ADE (eV)	VDE (eV)	vib freq ( $\text{cm}^{-1}$ )
$\text{Au}_2\text{O}_2^-$	X	3.03 (4)	3.29 (5)	1360 (70)
	A	3.86 (4)	4.01 (5)	1250 (70)
	B	4.32 (5)	$\sim 4.54$	$\sim 700$
	Au		4.84 (4)	
$\text{Au}_4\text{O}_2^-$	X	3.53 (5)	3.78 (5)	1360 (80)
	A		4.37 (5)	
	Au		4.81 (4)	
$\text{Au}_6\text{O}_2^-$	X	3.17 (5)	3.61 (5)	1330 (100)
	A	4.01 (5)	4.15 (5)	1100 (80)
	B	4.48 (5)	$> 4.48$	
	Au		4.83 (4)	

<sup>a</sup> Numbers in parentheses represent the experimental uncertainties in the last digits.

those of free  $\text{O}_2^-$ , and the assignment of the B band in the spectra of the  $n = 2$  and 6 species in the current study is sound.

From the vibrationally resolved spectra, the vertical detachment energy (VDE) for the ground-state transition in each case is readily obtained from the most intense vibrational peak, as summarized in Table 1, where the ground-state vibrational frequencies are also given. However, the vibrational peaks of band X in each spectrum show a width of about 120–140 meV, which is much larger than the instrumental resolution. This large spectral width can be due to either contributions from unresolved low-frequency vibrational modes or lifetime broadening. Therefore, the ground-state adiabatic detachment energy (ADE) is estimated by drawing a straight line along the leading edge of the first vibrational peak in each case and then adding the instrumental resolution to the intersection with the binding energy axis. The obtained ADE values are also given in Table 1 for  $\text{Au}_n\text{O}_2^-$  ( $n = 2, 4, 6$ ).

**3.2.  $\text{AuO}_2^-$ .** The 193 nm spectra of  $\text{AuO}_2^-$  are shown in Figure 3 at different source conditions and compared with that of  $\text{Au}^-$ . The spectrum in Figure 3a is obtained with a 1%  $\text{N}_2\text{O}$ -seeded He carrier gas. This spectrum is entirely due to the linear  $\text{OAUO}^-$  dioxide, which has been studied in detail in a recent



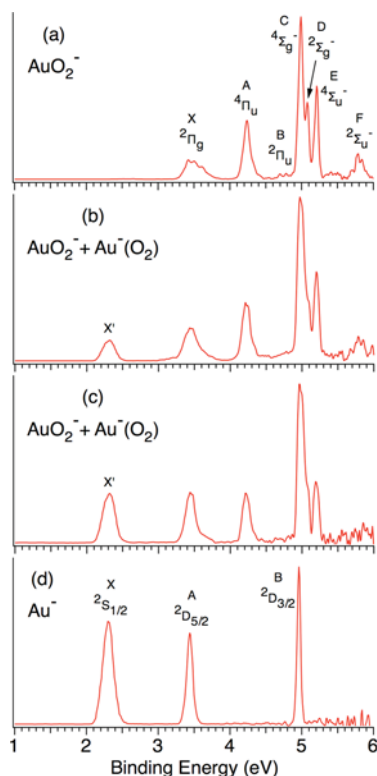


**Figure 3.** Photoelectron spectra of  $AuO_2^-$  at 193 nm in comparison with that of  $Au^-$ . (a) Spectrum of  $AuO_2^-$  dioxide using a  $N_2O/He$  carrier gas; the assignments are from ref 26. (b and c) Spectra of  $AuO_2^-$  using an  $O_2/He$  carrier gas, showing contributions of the  $Au^-(O_2)$  van der Waals complex, whose intensities increase with better cooling from (b) to (c).

joint PES and *ab initio* study.<sup>26</sup> The spectral assignments obtained from the previous study are given in Figure 3a. The spectrum shown in Figure 3b is measured for  $AuO_2^-$  produced using 5%  $O_2/He$  as the carrier gas. This spectrum is different from the data in Figure 3a: an extra peak ( $X'$ ) around 2.3 eV is observed and at the same time the relative intensity of the X band for the  $AuO_2^-$  dioxide appears to be enhanced. As we increase the cooling effect of the cluster source, we observe the relative intensity of the  $X'$  band increases (Figure 3c).

As described previously,<sup>25</sup> the cluster temperatures from our source depend on the residence time inside the cluster nozzle. The longer the residence time, the colder the clusters. We can tune the residence time or the relative cluster temperatures by varying the delay time of the cluster extraction for mass analyses with respect to the firing of the vaporization laser. A smaller delay time implies a short residence time or hot clusters. In Figure S1, we show a series of spectra for  $AuO_2^-$  produced with the 5%  $O_2/He$  carrier gas at different residence times. We observe that under hot conditions only the  $AuO_2^-$  dioxide isomer is produced. As we increase the residence time, the extra peak gradually appears and becomes very strong at the longest residence time. These observations suggest that the extra peak comes from a weakly bound or physisorbed  $Au^-(O_2)$  complex. Indeed, the  $X'$  peak of  $Au^-(O_2)$  is nearly the same as that of  $Au^-$  (Figure 3d). The second and third peaks from the  $Au^-(O_2)$  complex should also be similar to those (A and B) of  $Au^-$ , and they overlap with the X and C bands of  $AuO_2^-$  dioxide,

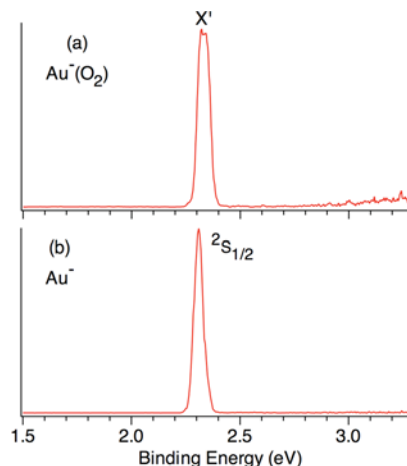


**Figure 4.** Photoelectron spectrum of the  $Au^-(O_2)$  van der Waals complex at 355 nm (3.496 eV) in comparison with that of  $Au^-$ .

**Table 2.** Observed Adiabatic Detachment Energies (ADE) of Physisorbed  $O_2$  Complexes for the Odd-Sized Clusters,  $Au_n^-(O_2)$  ( $n = 1, 3, 5, 7$ ), Compared with Those of the Corresponding Free  $Au_n^-$  Clusters<sup>a</sup>

$Au_n^-(O_2)$	ADE	$Au_n^-$	ADE <sup>b</sup>	$\Delta E^c$
1	2.322 (10)	1	2.30863	0.013
3	3.89 (1)	3	3.88 (2)	0.01
5	3.10 (2)	5	3.08 (3)	0.02
7	3.42 (3)	7	3.42 (3)	~0

<sup>a</sup> All values are in eV. Numbers in parentheses represent the uncertainties in the last digits. <sup>b</sup> The ADE of  $Au^-$  is from ref 36, and those for the larger clusters are from ref 27. <sup>c</sup> Shift of the ADE of  $Au_n^-(O_2)$  relative to that of  $Au_n^-$ .

respectively, as can be seen by comparing Figure 3, c and d. We further measured the spectrum of the physisorbed  $Au^-(O_2)$  complex with enhanced resolution at 355 nm (Figure 4a), which displays unresolved fine features. The ADE of  $Au^-(O_2)$  is measured to be 2.322 eV (Table 2), which is slightly higher than that of  $Au^-$  (2.3086 eV) and is consistent with the weakly bound nature of  $Au^-(O_2)$ .

**3.3.  $Au_3O_2^-$ .** The 193 nm spectra of  $Au_3O_2^-$  under different source conditions are compared with that of bare  $Au_3^-$  in Figure 5. The spectrum shown in Figure 5b was obtained for  $Au_3O_2^-$  using a 1%  $N_2O/He$  carrier gas under similar conditions to those for the  $AuO_2^-$  dioxide spectrum in Figure 3a. This spectrum displays extremely high electron-binding energies, with the VDE of the X band being 4.32 eV. Similar to the  $AuO_2^-$  dioxide, this  $Au_3O_2^-$  species must be also in the dioxide form. The spectrum in Figure 5c was obtained by using the 0.5%  $O_2/He$  carrier gas. The  $Au_3O_2^-$  system behaves similarly to  $AuO_2^-$ : in addition to the dioxide form, a weak low-binding energy peak ( $X'$ , Figure 5c) appears at ~3.9 eV. The binding energy of this peak is very similar to that of bare  $Au_3^-$ , suggesting that this peak comes from a physisorbed  $Au_3^-(O_2)$  similar to  $Au^-(O_2)$ . However, the relative intensity of the  $Au_3^-(O_2)$  complex is always weak even under the coldest source conditions. In Figure 6, we compare the 266 nm spectra of  $Au_3O_2^-$  and  $Au_3^-$  under higher spectral resolution. The relative intensity of the  $X'$  band is much enhanced. The ADE of the  $Au_3^-(O_2)$  complex is measured to be 3.89 eV (Table 2), slightly blue-shifted relative to that of  $Au_3^-$  (3.88 eV), consistent with the weakly bonded nature of  $Au_3^-(O_2)$ . The A band of  $Au_3^-$  exhibited a dramatic photon energy dependence, and its relative intensity was

(26) Zhai, H. J.; Burgel, C.; Bonacic-Koutecky, V.; Wang, L. S. *J. Am. Chem. Soc.* **2008**, *130*, 9156.

(27) Hakkinen, H.; Yoon, B.; Landman, U.; Li, X.; Zhai, H. J.; Wang, L. S. *J. Phys. Chem. A* **2003**, *107*, 6168.

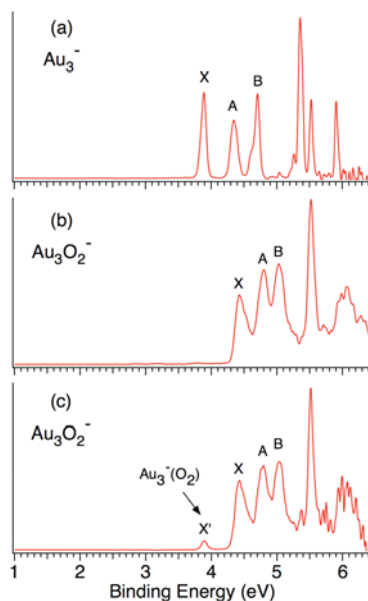


**Figure 5.** Photoelectron spectra of  $\text{Au}_3\text{O}_2^-$  at 193 nm in comparison with that of  $\text{Au}_3^-$  (a). (b) Spectrum of  $\text{Au}_3\text{O}_2^-$  using a  $\text{N}_2\text{O}/\text{He}$  carrier gas. (c) Spectrum of  $\text{Au}_3\text{O}_2^-$  using an  $\text{O}_2/\text{He}$  carrier gas, showing contributions from a weakly bonded  $\text{Au}_3^-(\text{O}_2)$  complex.

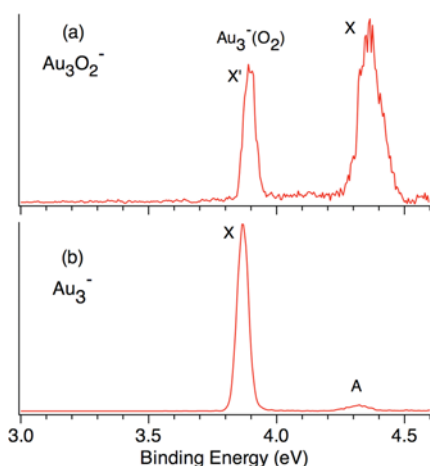


**Figure 6.** Photoelectron spectrum of the weakly bonded  $\text{Au}_3^-(\text{O}_2)$  complex at 355 nm in comparison with that of  $\text{Au}_3^-$ .

significantly reduced at 266 nm (Figure 6b), as pointed out previously.<sup>27</sup>

**3.4.  $\text{Au}_5\text{O}_2^-$  and  $\text{Au}_7\text{O}_2^-$ .** The spectra of  $\text{Au}_5\text{O}_2^-$  and  $\text{Au}_7\text{O}_2^-$  at two different photon energies are compared with their parent gold clusters in Figures 7 and 8, respectively. We observe the spectra of  $\text{Au}_5\text{O}_2^-$  and  $\text{Au}_7\text{O}_2^-$  to be nearly identical to their respective parent gold clusters. Even the ADE of each  $\text{O}_2$  complex displays no measurable shift from its parent gold clusters within our experimental uncertainties (Table 2). These observations suggest that these two clusters exist in the form of weakly bonded van der Waals complexes,  $\text{Au}_5^-(\text{O}_2)$  and  $\text{Au}_7^-(\text{O}_2)$ , in which  $\text{O}_2$  exerts little perturbation to the parent gold clusters. We have also produced van der Waals clusters of  $\text{Au}_n^-$  with Ar and obtained their PES spectra, which are all identical to those of the parent gold clusters with little spectral shift.<sup>28</sup> There are some very weak signals in the spectra of the  $\text{O}_2$  complexes, notably between 3.5 and 4.0 eV in the case of  $\text{Au}_5^-(\text{O}_2)$  (Figure 7a) and between 4.0 and 4.4 eV in the case of  $\text{Au}_7^-(\text{O}_2)$  (Figure 8a). These weak signals could come from

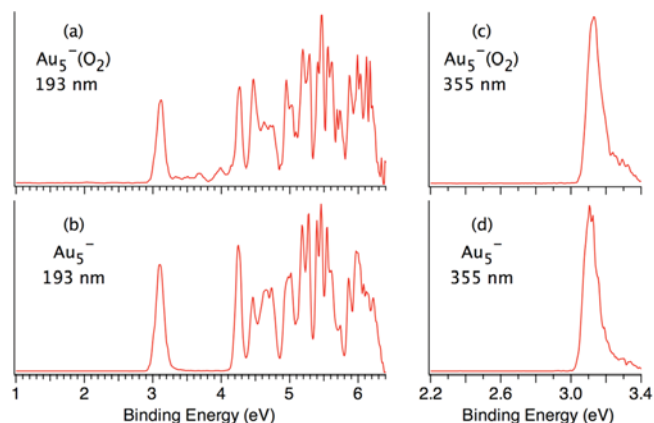


**Figure 7.** Photoelectron spectra of weakly bonded  $\text{Au}_5^-(\text{O}_2)$  complex at 193 and 355 nm in comparison with those of  $\text{Au}_5^-$ .

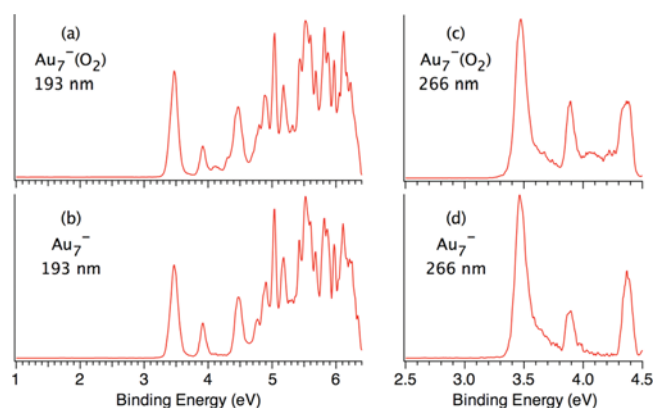


**Figure 8.** Photoelectron spectra of weakly bonded  $\text{Au}_7^-(\text{O}_2)$  complex at 193 and 355 nm in comparison with those of  $\text{Au}_7^-$ .

minor populations of the dioxide isomers. However, using the  $\text{N}_2\text{O}/\text{He}$  carrier gas, we observed negligible intensities for the dioxides in these cases.

## 4. Discussion

**4.1. Physisorption of  $\text{O}_2$  to Odd-Sized  $\text{Au}_n^-$  ( $n = 1, 3, 5, 7$ ) Clusters.** The observation of physisorbed  $\text{Au}_n^-(\text{O}_2)$  complexes for the odd-sized clusters is a vivid demonstration of the inertness of these closed-shell gold cluster anions toward  $\text{O}_2$ . The dioxide isomers of  $\text{AuO}_2^-$  and  $\text{Au}_3\text{O}_2^-$  are formed, respectively, by reactions of  $\text{Au}^-$  and  $\text{Au}_3^-$  with O atoms, which can be produced in the laser vaporization plasma. This conclusion is confirmed by the laser experiment using  $\text{N}_2\text{O}$  as the oxygen source. Although the  $\text{AuO}_2^-$  dioxide is more stable than the  $\text{Au}^-(\text{O}_2)$  complex, it cannot be formed by direct reactions of  $\text{Au}^-$  with  $\text{O}_2$ . Jena and co-workers showed using DFT calculations that there is a 3 eV barrier for the  $\text{Au}^- + \text{O}_2$  reaction to form the dioxide,<sup>15</sup> which cannot be overcome under thermal conditions. The physisorbed nature of the  $\text{Au}^-(\text{O}_2)$  complex has been recently studied in detail, showing that the  $\text{O}_2$  binding energy to  $\text{Au}^-$  is only about 0.03 eV (0.78 kcal/mol) at the CCSD(T) level and the complete basis set limit.<sup>29</sup> Bonacic-

- (28) (a) Huang, W.; Wang, L. S. *Phys. Chem. Chem. Phys.* **2009**, *11*, 2663. (b) Huang, W.; Wang, L. S. *Phys. Rev. Lett.* **2009**, *102*, 153401. (c) Huang, W.; Bulusu, S.; Pal, R.; Zeng, X. C.; Wang, L. S. *ACS Nano* **2009**, *3*, 1225. (29) Gao, Y.; Huang, W.; Woodford, J.; Wang, L. S.; Zeng, X. C. *J. Am. Chem. Soc.* **2009**, *131*, 9484.

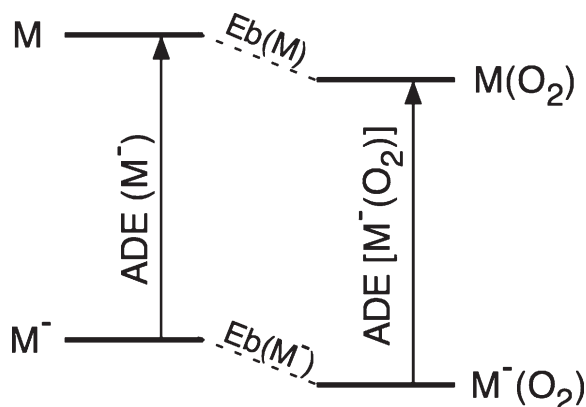


**Figure 9.** Schematics showing the relationship between adiabatic detachment energies (ADE) of anions and the O<sub>2</sub> binding energies (Eb) for a neutral and anion cluster.

Koutecky and co-workers have calculated the structure of the Au<sub>3</sub>O<sub>2</sub><sup>−</sup> dioxide,<sup>30</sup> which possesses a bent geometry and can be viewed as a Au<sub>2</sub> dimer end-bonded to a linear AuO<sub>2</sub><sup>−</sup> dioxide. Similar to the AuO<sub>2</sub><sup>−</sup> dioxide, the Au<sub>3</sub>O<sub>2</sub><sup>−</sup> dioxide is not formed by direct reactions of Au<sub>3</sub><sup>−</sup> with O<sub>2</sub>.

Previous DFT calculations suggest that the O<sub>2</sub> binding energies to the odd-sized Au<sub>n</sub><sup>−</sup> clusters (*n* = 3, 5, 7) range from 0.3 to 0.6 eV.<sup>21–23</sup> However, using the CCSD(T) level of theory the groups of Gordon and Metiu have shown that in fact O<sub>2</sub> does not bind to Au<sub>3</sub><sup>−</sup> and that DFT methods tend to overestimate the O<sub>2</sub> binding to gold clusters.<sup>23a</sup> The CCSD(T) result is confirmed by the current experimental observation: the Au<sub>3</sub><sup>−</sup>(O<sub>2</sub>) complex was difficult to observe, and it could be formed only under our coldest source conditions. For Au<sub>5</sub><sup>−</sup> and Au<sub>7</sub><sup>−</sup>, the O<sub>2</sub> binding must be also very weak because O<sub>2</sub> has very little effect on the electronic structures of the parent clusters. In particular, O<sub>2</sub> does not even induce a shift in the ADE of Au<sub>7</sub><sup>−</sup>(O<sub>2</sub>) relative to that of Au<sub>7</sub><sup>−</sup>, suggesting that the interactions between O<sub>2</sub> and Au<sub>7</sub><sup>−</sup> or Au<sub>7</sub> are similar and equally weak (Figure 9). As shown in Table 2, for *n* = 1, 3, 5, the O<sub>2</sub> binding induces a small blue shift in the ADEs of the Au<sub>n</sub><sup>−</sup>(O<sub>2</sub>) complexes relative to those of the bare clusters. These results imply that O<sub>2</sub> interacts with the anions slightly more strongly than with the corresponding neutral clusters, i.e., Eb(M<sup>−</sup>) > Eb(M) in Figure 9, because Eb(M<sup>−</sup>) = Eb(M) + ADE[M<sup>−</sup>(O<sub>2</sub>)] − ADE(M<sup>−</sup>). Available calculations in the literature are not consistent in predicting this binding energy trend from the anion to the neutral for the odd-sized clusters. In fact, the majority of the available calculations suggest that O<sub>2</sub> binds more strongly to the neutral odd-sized gold clusters than to the anions, inconsistent with the current experimental observations. As schematically shown in Figure 9, if O<sub>2</sub> were to bind more strongly to the neutral clusters, the observed ADEs for the Au<sub>n</sub><sup>−</sup>(O<sub>2</sub>) complexes should be smaller than those for their corresponding Au<sub>n</sub><sup>−</sup> clusters.

**4.2. Molecular Chemisorption of O<sub>2</sub> on Even-Sized Au<sub>n</sub><sup>−</sup> Clusters in Au<sub>n</sub>O<sub>2</sub><sup>−</sup> (*n* = 2, 4, 6).** From a careful saturation chemisorption study, Whetten and co-workers suggested that the interaction between even-sized Au<sub>n</sub><sup>−</sup> clusters and O<sub>2</sub> is via a one-electron charge transfer,<sup>10c</sup> yielding adsorbed superoxide complexes, Au<sub>n</sub>(O<sub>2</sub><sup>−</sup>). The observation of O–O vibrational structures in the PES of Au<sub>n</sub>O<sub>2</sub><sup>−</sup> (*n* = 2, 4, 6) by Gantefor and

co-workers confirmed this interpretation.<sup>14</sup> In the current study, we observed clearly three electronic transitions in the case of Au<sub>2</sub>O<sub>2</sub><sup>−</sup> (X, A, B), which are due to the O<sub>2</sub><sup>−</sup> moiety. These three bands are in fact reminiscent of the photoelectron spectrum of free O<sub>2</sub><sup>−</sup>,<sup>31</sup> providing further electronic structure evidence for the charge transfer interaction in the even-sized Au<sub>n</sub>O<sub>2</sub><sup>−</sup> clusters.

Free molecular O<sub>2</sub> possesses an open-shell triplet <sup>3</sup>Σ<sub>g</sub><sup>−</sup> ground state with the antibonding π<sub>g</sub> orbital half-filled (π<sub>g</sub><sup>2</sup>). In O<sub>2</sub><sup>−</sup>, the extra electron enters the π<sub>g</sub> orbital, resulting in the <sup>2</sup>Π<sub>g</sub> ground state for O<sub>2</sub><sup>−</sup> (π<sub>g</sub><sup>3</sup>). Photodetachment from O<sub>2</sub><sup>−</sup> results in the triplet <sup>3</sup>Σ<sub>g</sub><sup>−</sup> ground state and two low-lying excited singlet states for O<sub>2</sub>, <sup>1</sup>Δ<sub>g</sub> and <sup>1</sup>Σ<sub>g</sub><sup>+</sup>, with excitation energies at 0.982 and 1.636 eV, respectively.<sup>31</sup> As shown in Figure 2a and Table 1, the 266 nm PES spectrum of Au<sub>2</sub>O<sub>2</sub><sup>−</sup> yields excitation energies of 0.83 and 1.29 eV for the A and B bands, respectively. Different from those reported by Gantefor et al., the current higher resolution data show that the vibrational frequencies and the excitation energies in all three systems are nearly identical, as shown in Figure S2, where the 266 nm spectra of Au<sub>n</sub>O<sub>2</sub><sup>−</sup> (*n* = 2, 4, 6) are aligned for comparison. Note that only two O<sub>2</sub>-derived PES bands (X and A) are observed for Au<sub>4</sub>O<sub>2</sub><sup>−</sup> at 266 nm (Figure 2b) because of its high electron-binding energies. Another interesting observation is that the onsets of the Au-derived PES features are identical for all three systems (4.81–4.83 eV) within our experimental uncertainty, as seen in Figure 1a–c.

**4.3. On the Inconsistency of the Observed O–O Vibrational Frequencies in the PES Spectra of the Even-Sized Au<sub>n</sub>O<sub>2</sub><sup>−</sup> (*n* = 2, 4, 6) Clusters and the Expected Inertness of the Corresponding Neutral Au<sub>n</sub> Clusters with O<sub>2</sub>.** Previous experimental studies have shown that the closed-shell odd-sized Au<sub>n</sub><sup>−</sup> clusters do not react with O<sub>2</sub>.<sup>10</sup> Our current observations of weakly bonded O<sub>2</sub> complexes of these clusters provide direct spectroscopic evidence for the inertness of the odd-sized Au<sub>n</sub><sup>−</sup> clusters toward O<sub>2</sub>. The closed-shell Au<sub>n</sub><sup>−</sup> clusters possess relatively high electron-binding energies, making it energetically unfavorable for the charge transfer reaction to O<sub>2</sub>. Besides the high electron-binding energies, the spin selection rule also makes the closed-shell Au<sub>n</sub><sup>−</sup> clusters unfavorable to react with O<sub>2</sub>, which has a triplet ground state as mentioned above. A recent study has shown that closed-shell aluminum Al<sub>n</sub><sup>−</sup> cluster anions react much more slowly with O<sub>2</sub>, but their reactivity is considerably enhanced with singlet O<sub>2</sub> (<sup>1</sup>Δ<sub>g</sub>).<sup>32a</sup> Interestingly, both the global minimum *D*<sub>3h</sub> Au<sub>10</sub><sup>−</sup> and the Au<sub>16</sub><sup>−</sup> cage are known to be unreactive to O<sub>2</sub>.<sup>10,28a</sup> They are exceptions to the even–odd effect in the Au<sub>n</sub><sup>−</sup> reactivity with O<sub>2</sub>, although they possess the same spin state as the other reactive even-sized Au<sub>n</sub><sup>−</sup> clusters. These two clusters possess high electron-binding energies as a result of their corresponding neutrals being open-shell triplet states.<sup>27,33</sup> Again, the spin selection rule may also play a role in the nonreactivity of Au<sub>10</sub><sup>−</sup> and Au<sub>16</sub><sup>−</sup> with O<sub>2</sub>. Recently, we have observed a weakly bonded Au<sub>10</sub><sup>−</sup>(O<sub>2</sub>) complex, which yields a PES spectrum identical to that of the parent *D*<sub>3h</sub> Au<sub>10</sub><sup>−</sup> and confirms the inertness of Au<sub>10</sub><sup>−</sup> toward O<sub>2</sub>.<sup>28a</sup>

(30) Kimble, M. L.; Moore, N. A.; Johnson, G. E.; Castleman, A. W.; Burgel, C.; Mitric, R.; Bonacic-Koutecky, V. *J. Chem. Phys.* **2006**, *125*, 204311.

(31) Buntine, M. A.; Lavrich, D. J.; Dessent, C. E.; Scarton, M. G.; Johnson, M. A. *Chem. Phys. Lett.* **1993**, *216*, 471.

(32) (a) Burgert, R.; Schnockel, H.; Grubisic, A.; Li, X.; Stokes, S. T.; Bowen, K. H.; Gantefor, G. F.; Kiran, B.; Jena, P. *Science* **2008**, *319*, 438. (b) Reber, A. C.; Khanna, S. N.; Roach, P. J.; Woodward, W. H.; Castleman, A. W. *J. Am. Chem. Soc.* **2007**, *129*, 16098.

(33) Bulusu, S.; Li, X.; Wang, L. S.; Zeng, X. C. *Proc. Natl. Acad. Sci. U.S.A.* **2006**, *103*, 8326.



Analogously, the closed-shell neutral  $\text{Au}_n$  clusters ( $n = 2, 4, 6$ ) are not expected to react with  $\text{O}_2$  because the electron-binding (ionization) energies in these neutral clusters are much higher than those for the closed-shell odd-sized  $\text{Au}_n^-$  cluster anions. In other words, the neutral closed-shell  $\text{Au}_n$  clusters should form only weakly bonded physisorbed complexes with  $\text{O}_2$ . This conclusion is clearly inconsistent with the PES spectra of  $\text{Au}_n\text{O}_2^-$ , which yield spectroscopic information about the neutral  $\text{Au}_n\text{O}_2$  final states. The O–O vibrational frequency of  $1360\text{ cm}^{-1}$  observed in the PES spectra for the ground states of all three  $\text{Au}_n\text{O}_2$  systems is significantly smaller than that for free  $\text{O}_2$  ( $1580\text{ cm}^{-1}$ ). The vibrational frequency of the superoxide ion,  $\text{O}_2^-$ , is  $1090\text{ cm}^{-1}$ .<sup>34</sup> The  $1360\text{ cm}^{-1}$  vibrational frequency observed for the ground states of neutral  $\text{Au}_n\text{O}_2$  complexes is between those of the free  $\text{O}_2$  and  $\text{O}_2^-$ , suggesting significant chemical interactions between  $\text{Au}_n$  and  $\text{O}_2$  in the final  $\text{Au}_n\text{O}_2$  states, accessed in the photodetachment transitions.

As discussed in the Introduction, previous calculations have also shown that neutral  $\text{Au}_n$  clusters do not activate  $\text{O}_2$ . Then, the question is, how does one understand the reduced O–O vibrational frequency in the neutral  $\text{Au}_n\text{O}_2$  final states in the photodetachment experiment of  $\text{Au}_n\text{O}_2^-$  ( $n = 2, 4, 6$ )?

**4.4. Access of Excited States in PES of  $\text{Au}_n\text{O}_2^-$  ( $n = 2, 4, 6$ ).** According to our experimental observation of the weakly bonded nature of the closed-shell anions, the interactions between the even-sized  $\text{Au}_n$  clusters and  $\text{O}_2$  should be extremely weak and should be represented by a shallow van der Waals well. The O–O vibrational frequencies in the weakly bonded  $\text{Au}_n(\text{O}_2)$  complexes should be close to that of free  $\text{O}_2$ . Since PES is a vertical process, it may not be able to access the ground-state van der Waals potential curve of  $\text{Au}_n(\text{O}_2)$ . A detachment transition to the van der Waals well would be a bound-to-unbound transition, which should yield very broad and diffused PES bands. Instead, the observed PES spectra suggest bound-to-bound transitions, which could result only from transitions to excited states of  $\text{Au}_n\text{O}_2$ . This observation suggests that the interactions between  $\text{Au}_n$  and  $\text{O}_2$  may correspond to a double-well potential with a shallow ground-state van der Waals well at long  $\text{Au}_n\text{--O}_2$  distances and a deeper well at closer  $\text{Au}_n\text{--O}_2$  distances, but at a higher energy. The higher energy, deeper well can result from interactions of  $\text{Au}_n$  with an excited state of  $\text{O}_2$  and an avoided curve crossing with the ground-state van der Waals well, resulting in the putative double-well potential for  $\text{Au}_n\text{O}_2$ , as schematically shown in Figure 10.

The excited state could come from the interaction of  $\text{Au}_n$  with singlet  $\text{O}_2$  ( $^1\Delta_g$ ) (Figure 10), which is well known to be much more reactive than the ground-state triplet  $\text{O}_2$  ( $^3\Sigma_g^-$ ).<sup>35</sup> In addition, the spin-state selection rule is also fulfilled between the reactions of the singlet  $\text{O}_2$  and the closed-shell  $\text{Au}_n$  clusters. The first detachment channel reaching the  $\text{Au}_n\text{--O}_2(^1\Delta_g)$  final state can be understood from the following consideration. In the  $\text{Au}_n(\text{O}_2^-)$  complexes, the degeneracy of the  $\pi_g$  orbital in the  $\text{O}_2^-$  moiety is expected to be lifted, resulting in two nondegenerate orbitals: a fully occupied orbital ( $a^2$ ) and a singly occupied orbital (SOMO) ( $b^1$ ), as schematically shown in Figure 11a. A single electron detachment from the SOMO of  $\text{Au}_n(\text{O}_2^-)$  would result in a final state of  $\text{Au}_n(\text{O}_2)$  corresponding to the  $^1\Delta_g$  state of free  $\text{O}_2$ , as schematically shown in Figure 11b. Detachment of a spin-down electron from the  $a^2$  orbital would result in a

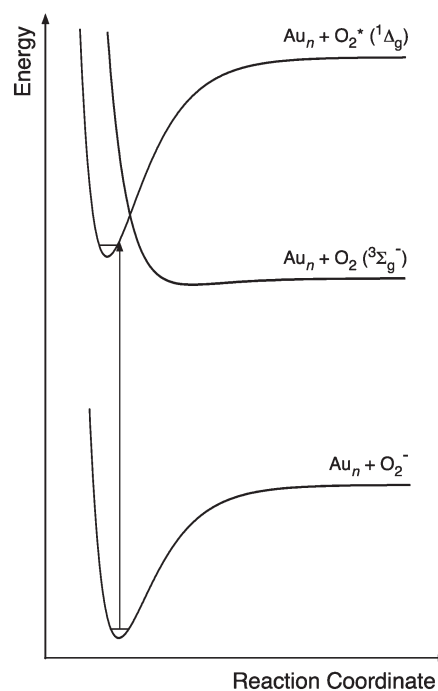


**Figure 10.** Schematic potential energy curves illustrating vertical detachment transitions from the ground state of  $\text{Au}_n\text{O}_2^-$  ( $n = 2, 4, 6$ ) to the final neutral states of  $\text{Au}_n\text{O}_2$ . Note the curve crossing between the ground-state van der Waals well and the deeper well between  $\text{Au}_n$  and the singlet  $\text{O}_2$  ( $^1\Delta_g$ ), which would result in a double well due to avoided curve crossing.

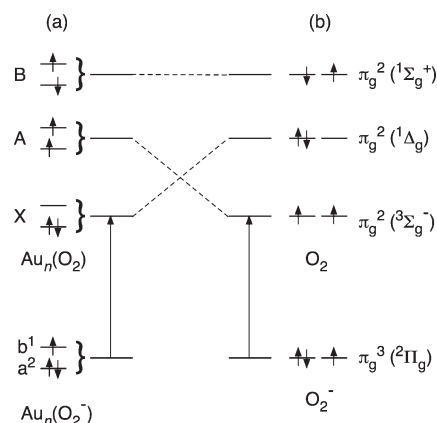


**Figure 11.** Schematics correlating single electron detachment from the  $\text{O}_2^-$  moiety in  $\text{Au}_n\text{O}_2^-$  ( $n = 2, 4, 6$ ) with those from free  $\text{O}_2^-$ .

triplet final state in  $\text{Au}_n(\text{O}_2)$ , which should correspond to the  $^3\Sigma_g^-$  state of free  $\text{O}_2$ . This detachment channel should reach the repulsive part of the ground-state  $\text{Au}_n\text{--O}_2$  van der Waals well (Figure 10), corresponding to the A band in the PES spectra. The observed vibrational structures in the A band suggest a transition to a bound state, which is likely derived from the avoided curve crossing with the potential energy curve from the  $^1\Delta_g$  state of  $\text{O}_2$ . The detachment of a spin-up electron from the  $a^2$  orbital should lead to a final state corresponding to the  $^1\Sigma_g^+$  state of free  $\text{O}_2$  (Figure 11).

The deeper well in the double-well potential in  $\text{Au}_n(\text{O}_2)$  is unstable, and predissociation occurs to the ground state. This is consistent with our observed 266 nm photoelectron spectra (Figure 2), in which the resolved vibrational peaks are all much broader than the instrumental resolution. While this broadening can be due to unresolved low-frequency vibrational modes, one

(34) NIST Chemistry WebBook: <http://webbook.nist.gov/chemistry>.

(35) Schweitzer, C.; Schmidt, R. *Chem. Rev.* **2003**, *103*, 1685.

(36) Riestra-Kiracife, J. C.; Tschumper, G. S.; Schaefer, H. F.; Nandi, S.; Ellison, G. B. *Chem. Rev.* **2002**, *102*, 231.

possibility would be lifetime broadening due to predissociation to the ground state, providing evidence for the proposed interpretation.

*Ab initio* calculations at the CCSD(T) level showed that DFT calculations tend to overestimate the Au<sub>n</sub><sup>−</sup>/O<sub>2</sub> binding by as much as 0.5 eV,<sup>23a</sup> which is on the order of the interactions between gold clusters and O<sub>2</sub>. Preliminary calculations by Jun Li (private communication) suggest that there is significant multireference character in the ground state wave function of Au<sub>2</sub>O<sub>2</sub><sup>−</sup>. Therefore, the interactions between O<sub>2</sub> and gold clusters are quite complicated. The current data should provide good benchmarks to calibrate theoretical methods that can properly treat the O<sub>2</sub> interactions with gold clusters. It would also be very interesting to investigate the reactivities of singlet oxygen with gold clusters to confirm the proposed double-well potential for the interactions of O<sub>2</sub> with neutral gold clusters.

## 5. Conclusions

In conclusion, we present a systematic PES study of the Au<sub>n</sub>O<sub>2</sub><sup>−</sup> (*n* = 1–7) cluster complexes. Well-resolved photoelectron spectra are obtained for the even-sized Au<sub>n</sub>O<sub>2</sub><sup>−</sup> (*n* = 2, 4, 6) clusters, confirming the molecular chemisorption nature of O<sub>2</sub> in these systems. Both the electron-binding energies and O–O vibrational frequencies are more accurately measured. Physisorbed Au<sub>n</sub><sup>−</sup>(O<sub>2</sub>) complexes are observed for the odd-sized Au<sub>n</sub>O<sub>2</sub><sup>−</sup> (*n* = 1, 3, 5, 7) clusters for the first time, confirming the inertness of the odd-sized Au<sub>n</sub><sup>−</sup> clusters toward O<sub>2</sub>. The inconsistency of the observed O–O vibrational frequency with

the expected inertness of the even-sized *neutral* Au<sub>n</sub> clusters toward O<sub>2</sub> is discussed. It is suggested that photodetachment from the molecularly chemisorbed Au<sub>n</sub>(O<sub>2</sub><sup>−</sup>) complexes cannot access the ground-state van der Waals potential curves of the *neutral* even-sized Au<sub>n</sub>(O<sub>2</sub>) complexes. A double-well potential is proposed for the Au<sub>n</sub>–O<sub>2</sub> interaction, which consists of a lower energy, shallow van der Waals well at long Au<sub>n</sub>–O<sub>2</sub> distances and a higher energy, deeper well at shorter Au<sub>n</sub>–O<sub>2</sub> distances. The double-well potential is suggested to result from a putative avoided curve crossing between the ground-state van der Waals well and the deeper well derived from interactions of Au<sub>n</sub> with singlet O<sub>2</sub> (<sup>1</sup>Δ<sub>g</sub>). Clearly more accurate theoretical calculations are needed to understand the PES spectra and the detailed interactions between O<sub>2</sub> and gold clusters. Such understanding is important for elucidating the catalysis of supported gold nanoparticles, in which the activation of O<sub>2</sub> is the most important step.

**Acknowledgment.** We thank Professors Jun Li, Mingfei Zhou, and Manfred Kappes for valuable discussions. This research was supported by the National Science Foundation (CHE-0749496).

**Supporting Information Available:** Photoelectron spectra of AuO<sub>2</sub><sup>−</sup> at 193 nm under different experimental conditions and comparison of the fine features in the 266 nm photoelectron spectra of Au<sub>n</sub>(O<sub>2</sub><sup>−</sup>) (*n* = 2, 4, 6). This material is available free of charge via the Internet at <http://pubs.acs.org>.

JA910401X